Thermodynamic and Structural Consequences of Changing a Sulfur Atom to a Methylene Group in the M13Nle Mutation in Ribonuclease-S[†,Δ]

James Thomson,[‡,§] Girish S. Ratnaparkhi,[‖] Raghavan Varadarajan,[‖] Julian M. Sturtevant,[‡,⊥] and Frederic M. Richards*[,⊥]

Departments of Chemistry and of Molecular Biochemistry and Biophysics, Yale University, New Haven, Connecticut 06511, and Molecular Biophysics Unit, Indian Institute of Science, Bangalore, India

Received March 3, 1994; Revised Manuscript Received May 9, 1994[⊕]

ABSTRACT: Two fragments of pancreatic ribonuclease A, a truncated version of S-peptide (residues 1–15) and S-protein (residues 21–124), combine to give a catalytically active complex. We have substituted the wild-type residue at position 13, methionine (Met), with norleucine (Nle), where the only covalent change is the replacement of the sulfur atom with a methylene group. The thermodynamic parameters associated with the binding of this variant to S-protein, determined by titration calorimetry in the temperature range 10–40 °C, are reported and compared to values previously reported [Varadarajan, R., Connelly, P. R., Sturtevant, J. M., & Richards, F. M. (1992) *Biochemistry 31*, 1421–1426] for other position 13 analogs. The differences in the free energy and enthalpy of binding between the Met and Nle peptides are 0.6 and 7.9 kcal/mol at 25 °C, respectively. These differences are slightly larger than, but comparable to, the differences in the values for the Met/Ile and Met/Leu pairs. The structure of the mutant complex was determined to 1.85 Å resolution and refined to an *R*-factor of 17.4% The structures of mutant and wild-type complexes are practically identical although the Nle side chain has a significantly higher average *B*-factor than the corresponding Met side chain. In contrast, the *B*-factors of the atoms of the cage of residues surrounding position 13 are all somewhat lower in the Nle variant than in the Met wild-type. Thus, the large differences in the binding enthalpy appear to reside entirely in the difference in chemical properties or dynamic behavior of the -S- and -CH_2- groups and not in differences in the geometry of the side chains or the internal cavity surface. In addition, a novel method of obtaining protein stability data by means of isothermal titration calorimetry is introduced.

The side chains of leucine, isoleucine, norleucine, and methionine all have nearly identical volumes and surface areas. The first three differ only in the position of a methyl group. Norleucine and methionine differ only in the substitution of a divalent sulfur atom for a methylene group. The two amino acid side chains have the same chain length and the same number of single rotatable bonds.

In an earlier study of the association of S-peptide[1] variants and S-protein in the ribonuclease-S system (Connelly et al., 1990; Varadarajan and Richards, 1992), it was found that substitution of the wild-type methionine at position 13 with either leucine or isoleucine unsurprisingly produced little or no change in the free energy of association of the peptide and protein. In the particular context of the cavity surrounding position 13, the shape differences between these residues were unimportant. However, a comparison of these same variants showed a difference of the order of 5.5 kcal/mol in the enthalpy of association between the methionine and the leucine and isoleucine peptides. Since this particular set is not isosteric, it was not possible to decide if the difference was due to the shape of the side chains or to the chemical difference between a sulfur atom and a methylene group. To investigate this matter further, we decided to examine both the thermodynamic and structural consequences of replacing Met13 with norleucine, where the only covalent change is the replacement of a sulfur atom with a methylene group.

MATERIALS AND METHODS

Materials. RNase-S was obtained from Sigma. S-protein was purified from RNase-S either by the method of Doscher and Hirs (1967) or by reverse-phase FPLC on a C_{18} column using a 0–40% acetonitrile gradient with 0.1% TFA. Bakerbond prepscale C_{18} resin was obtained from J. T. Baker. M13Nle is a C-terminal amidated S-peptide analog in which Met13 of the 15-residue truncated version of S-peptide was substituted by norleucine. This peptide was obtained from Multiple Peptide Systems Inc. (San Diego, CA). The crude peptide was purified by reverse-phase HPLC on a Vydak C_{18} column using a water/acetonitrile gradient containing 0.1% TFA. The samples were lyophilized 2–3 times from water to remove any traces of the solvent components. The low heats of dilution observed in the titration calorimetric experiments suggested that there were no residual solvent components. Purified S-protein and the peptide were lyophilized and stored at −20 °C. The concentration of stock peptide solutions was determined by quantitative amino acid analysis at Yale University Medical School Protein and Nucleic Acid Chemistry Facility prior to lyophilization as described earlier (Connelly et al., 1990).

[†] Supported by National Institute of General Medical Sciences Grants GM-22778 and GM-04725, National Science Foundation Grant MCB-9120192, and, at the Indian Institute of Science, CSIR Grant 37(0813)/93/EMRII. G.S.R. is a Junior Research Fellow of CSIR.

[Δ] Coordinates have been deposited in the Brookhaven Protein Data Bank under the file name 1RLN.

[‡] Department of Chemistry, Yale University.

[§] Present address: Agouron Pharmaceuticals Inc., San Diego, CA, 92121.

[‖] Indian Institute of Science.

[⊕] Abstract published in *Advance ACS Abstracts,* June 15, 1994.

[⊥] Department of Molecular Biochemistry and Biophysics, Yale University.

[1] Abbreviations: RNase-A, bovine pancreatic ribonuclease; RNase-S, product of proteolytic cleavage of bond 20–21 in RNase-A; S-protein, residues 21–124 of RNase-S; S-peptide, residues 1–20 of RNase-S; S-15, truncated version of S-peptide (residues 1–15 with a C-terminal amide); Nle, norleucine; ANB, α-amino-*n*-butyric acid.

0006-2960/94/0433-8587$04.50/0

Table 1: Thermodynamic Parameters Obtained on Titrating S-Protein with the M13Nle S-Peptide Analog[a]

temp (°C)	n	ΔH_{obs} (kcal/mol)	K (M^{-1})	$\Delta G°$ [b] (kcal/mol)	$T\Delta S°$ [b] (kcal/mol)
10.0	1.03	−21.57 ± 0.09	2.5 (±0.2) × 10^7		
10.0	0.96	−21.69 ± 0.06	2.4 (±0.2) × 10^7		
		−21.69 ± 0.06	**2.45 (±0.05) × 10^7**	**−9.57 ± 0.013**	**−12.06 ± 0.06**
15.0	1.08	−25.12 ± 0.07	1.10 (±0.07) × 10^7		
15.0	1.03	−24.91 ± 0.08	1.30 (±0.09) × 10^7		
		−25.02 ± 0.11	**1.2 (±0.1) × 10^7**	**−9.33 ± 0.050**	**−15.69 ± 0.12**
20.0	1.08	−27.32 ± 0.16	5.6 (±0.5) × 10^6		
20.0	1.10	−27.28 ± 0.14	5.5 (±0.5) × 10^6		
		−27.30 ± 0.02	**5.55 (±0.05) × 10^6**	**−9.04 ± 0.008**	**−18.25 ± 0.02**
25.0	1.07	−33.49 ± 0.16	2.9 (±0.2) × 10^6		
25.0	1.09	−35.4 ± 0.2	2.6 (±0.2) × 10^6		
		−34.4 ± 1.0	**2.75 (±0.15) × 10^6**	**−8.78 ± 0.03**	**−25.6 ± 1.0**
30.0	1.10	−44.0 ± 0.3	1.40 (±0.12) × 10^6		
30.0	1.10	−44.5 ± 0.2	1.10 (±0.06) × 10^6		
		−44.3 ± 0.3	**1.25 (±0.15) × 10^6**	**−8.46 ± 0.008**	**−35.8 ± 0.3**
35.0	1.11	−55.0 ± 0.3	3.72 (±0.13) × 10^5		
35.0	1.08	−55.9 ± 0.3	3.32 (±0.11) × 10^5		
		−55.5 ± 0.5	**3.5 (±0.2) × 10^5**	**−7.82 ± 0.03**	**−47.7 ± 0.6**
40.0	1.01	−71.8 ± 1.0	5.35 (±0.16) × 10^4		
40.0	0.88	79 ± 3	5.6 (±0.2) × 10^4		
		−75 ± 4	**5.48 ± (0.13) × 10^4**	**−6.79 ± 0.015**	**−68 ± 4**

[a] Values reported are per mole of peptide. Errors on the fitted K and ΔH_{obs} are from the ORIGIN program. Average values for duplicate experiments are reported in boldface type. Errors on average values are reported as the deviation of the mean. Errors on $\Delta G°$ and $T\Delta S°$ were determined by propagation of errors. [b] Values calculated from average values of K and ΔH_{obs}.

S-Protein and S-peptide solutions used for the titration experiments were prepared by redissolving the lyophilized samples in an appropriate volume of buffer (50 mM acetate/100 mM NaCl, adjusted to pH 6.0 with 1 N HCl). After resuspension, the S-protein concentrations were verified spectroscopically using an extinction coefficient at 280 nm of 9.56 mM^{-1} cm^{-1} (Connelly et al., 1990).

Titration Calorimetry. The calorimetric experiments were performed using an OMEGA isothermal titration calorimeter from MicroCal Inc. (Northampton, MA). With the exception of increasing the interval between consecutive injections from 4.5 to 6 min for some of the experiments, the titrations were performed as previously described (Connelly et al., 1990; Varadarajan et al., 1990).

Titration Data Analysis. The method used for sample preparation does not ensure a perfect match of the pH of the sample solutions with that of the buffer. This can produce a small discrepancy between the sum of the heats of dilutions obtained from the dilution controls (i.e., from titrations of peptide into buffer, buffer in to S-protein, and buffer into buffer) and the heat of injection observed after virtual saturation of the system has been achieved. To circumvent this problem, the heat attributed to the dilution effects was treated as an additional variable. In all cases, the best fit of the titration data was achieved when a heat of dilution less than that derived experimentally was utilized. For example, for an initial heat of injection of 200 μcal, the estimated dilution correction from blank runs was −6.6 μcal; from the best-fit procedure, a correction of −2.4 μcal was obtained. Data were analyzed using the ORIGIN software package for the OMEGA calorimeter (distributed by MicroCal Inc.) assuming a single set of identical binding sites.

Wiseman et al. (1989) have pointed out that the reliability of the determination of the binding constant K_b depends upon the dimensionless quantity C which is the product of K_b and the initial concentration, $[M_T]_0$, of the macromolecule in the cell. They suggest that the macromolecule concentration should be adjusted such that a C value between 1 and 1000 is obtained. The experiments reported here cover the range of C values from approximately 20 to 700 with the exception of the 40 °C data where the C value was about 2.

Crystallization. Cesium chloride was obtained from Sigma Chemical Co. Ammonium sulfate and sodium acetate were obtained from Ranbaxy Chemicals (India). The S-protein–M13Nle peptide complex was prepared and crystallization was carried out at 20 °C as described by Varadarajan and Richards (1992). The final conditions in the drop were 4–5 mg/mL protein, 3 M CsCl, 0.1 M acetate buffer, pH 5.75, and 35% $(NH_4)_2SO_4$.

X-ray Data Collection, Refinement, and Structural Analysis. The crystals were stabilized in 75% $(NH_4)_2SO_4$ at pH 4.75 and the CsCl was washed out by repeated buffer changes. The size of the single crystal used for data collection was of the order of 0.6 × 0.5 × 0.3 mm. X-ray data were collected from the capillary-mounted crystal with a Siemens Xentronics area detector on a GEC GX20 rotating-anode generator operated at 36 kV and 39 mA at the Molecular Biophysics Unit, Indian Institute of Science. The beam was passed through a 0.5 mm collimator. Each frame was recorded for 475 s with a 0.25° sweep. The data were collected on a single crystal at room temperature, and reduced and averaged using the software provided (Howard et al., 1985).

The starting model used for the refinement was the complex of the wild-type peptide S15 with S-protein (Kim et al., 1992). Refinement, including addition of water, sulfate, and multiple conformations, was carried out using simulated annealing with the program X-PLOR (Brünger, 1992). Detailed descriptions of the refinement methodology can be found in Kim et al. (1992). In addition to unrestrained B-factor refinement described for the wild-type and other mutant complexes (Kim et al., 1992; Varadarajan & Richards, 1992), we also carried out restrained B-factor refinement using target standard deviations as follows: (1) 1.5 and 2.0 Å^2 for the B-factors for main and side chain 1–2 atom pairs; (2) 2.0 and 2.5 Å^2 for the B-factors for main and side chain 1–3 atom pairs. However, the calculated electron density maps were identical for restrained and unrestrained B-factor refinements. The average B-factors quoted in the next section refer to the values from the unrestrained B-factor refinement. All refinement calculations were carried out on IBM RS/6000 workstations at the Supercomputer Education and Research Center, Indian Institute of Science, and on a CONVEX C-2 at the Center

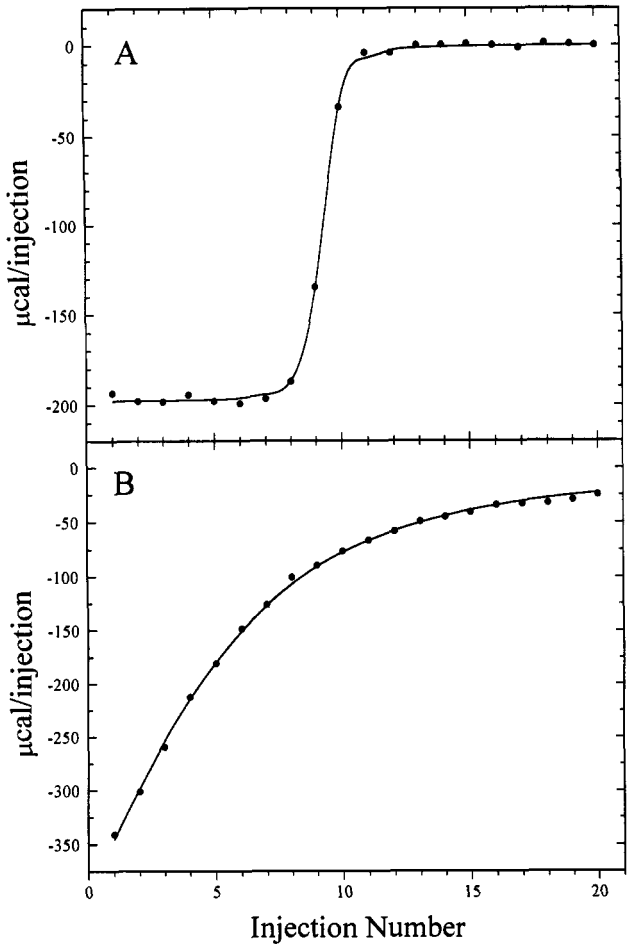

FIGURE 1: Calorimetric titrations of S-protein with the M13Nle peptide at (A) 15 °C ($K = 1.2 \times 10^7$ M^{-1}, C value = 689) and (B) 40 °C ($K = 5.6 \times 10^4$ M^{-1}, C value = 1.54). The solid line represents the best fit of the heat of injection versus the injection number using the ORIGIN software package (see Titration Data Analysis under Materials and Methods).

for Structural Biology, Yale University. $2F_o - F_c$ maps (contoured at 1.0 σ) and $F_o - F_c$ (contoured at ±2.5 σ) were examined, and manual adjustments to the model were made using the program FRODO (Jones, 1985) on a Silicon Graphics 4D/310VGX workstation at the Distributed Information Center, Indian Institute of Science. Calculations of van der Waals energies of interaction and accessible surface area were performed using the program X-PLOR. For the area calculations, several probe radii ranging in size from 0.8 to 1.6 Å were used.

RESULTS

Thermodynamic Data. The full set of data including error estimates for the titration of S-protein with the peptide M13Nle is listed in Table 1. As examples of the data quality, the titration curves with the highest and lowest C values, 689 and 1.54, respectively, are shown in Figure 1; these are the runs likely to have the largest errors. In both cases, the solid line was calculated using the values of the best-fit parameters listed in Table 1.

A plot of the total enthalpy of reaction, $\Delta H_{obs}(T)$, that accompanies the titration of S-protein with peptide, after correction for the heats of dilution, is shown in Figure 2 as a function of temperature. $\Delta H_{obs}(T)$ represents the sum of the heat of binding, $\Delta H_{bind}(T)$, of S-protein + peptide and the heats associated with the conformational changes that are

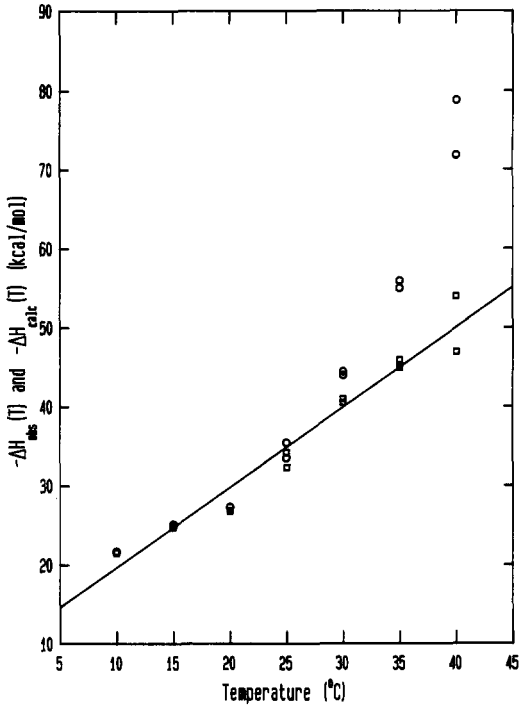

FIGURE 2: Total observed enthalpy of reaction, $\Delta H_{obs}(T)$ (○), taken from values in Table 1, and the calculated enthalpy of binding, $\Delta H_{calc}(T)$, (□), as a function of temperature. The $\Delta H_{calc}(T)$ values were obtained from eq 6 as described under Discussion. The line represents a linear least-squares fit to the $\Delta H_{calc}(T)$ data.

induced by the binding reaction, $\Delta H_{conf}(T)$:

$$\Delta H_{obs}(T) = \Delta H_{bind}(T) + \Delta H_{conf}(T) \quad (1)$$

(The conformational changes referred to in this study are restricted to those in the S-protein component of the reaction; see Discussion.) $\Delta H_{fold}(T)$ is the enthalpy of the unfolding reaction. We will assume that the heat capacity changes, $\Delta C_{p_{bind}}$, for the binding reaction and $\Delta C_{p_{fold}}$ for the full conformational change, a fraction of which will affect the binding reaction, are both temperature independent, but not necessarily numerically equal. Then:

$$\Delta H_{bind}(T) = \Delta H_{bind}(T_0) + \Delta C_{p_{bind}}(T - T_0) \quad (2)$$

and

$$\Delta H_{fold}(T) = \Delta H_{fold}(T_{1/2}) + \Delta C_{p_{fold}}(T - T_{1/2}) \quad (3)$$

where T is the temperature of interest, T_0 is the reference temperature, taken in this work to be 25 °C, and $T_{1/2}$ is the temperature of the midpoint of the folding transition. Assuming a two-state process:

$$\Delta H_{conf}(T) = f_u(T)\Delta H_{fold}(T) \quad (4)$$

where $f_u(T)$ is the fraction of the total S-protein in the unfolded form. The observed enthalpy, $\Delta H_{obs}(T)$, is then given by the combination of eq 1 through 4. The temperature dependencies of f_u and the two enthalpies may be expected to produce a quadratic dependence of ΔH_{obs} on temperature as seen in Figure 2.

The enthalpy changes in Table 1 for the 3 temperatures below 25 °C were fitted to a straight line. The slope and the intercept at 25 °C provided the values of ΔC_p and ΔH(25 °C) for the M13Nle S-peptide analog listed in Table 2. For comparison, the results for the S-peptide analogs studied

Table 2: Standard Enthalpy and Heat Capacity for Peptide Binding to S-Protein from Data in the Temperature Range 5–20 °C[a]

peptide	ΔH(25 °C) (kcal mol^{-1})	ΔC_P (kcal mol^{-1} K^{-1})
S15	−38.2	−0.76
M13I	−32.8	−0.55
M13L	−32.5	−0.66
M13Nle	**−30.3**	**−0.57**
M13A	−35.4	−0.96
M13ANB	−29.0	−0.59
M13V	−34.7	−0.59
M13F	−33.5	−0.73

[a] Data from this paper for M13Nle in boldface type. Data for the other peptides taken from Varadarajan et al. (1991), and modified as described in the text.

Table 3: Difference Thermodynamic Parameters (Relative to S15 S-Peptide) for Peptide Binding to S-Protein

peptide	$\Delta\Delta H$(25 °C)[a] (kcal mol^{-1})	$\Delta\Delta C_p$[a] (kcal mol^{-1} K^{-1})	$\Delta\Delta G°$(25 °C)[b] (kcal mol^{-1})	$T\Delta\Delta S°$(25 °C)[c] (kcal mol^{-1})
M13I	5.4	0.21	0.1	5.3
M13L	5.7	0.10	0.3	5.2
M13Nle	**7.9**	**0.19**	**0.8**	**7.1**
M13A	2.8	−0.20	4.3	−1.5
M13ANB	9.2	0.17	1.5	7.7
M13V	3.5	0.17	−0.1	3.6
M13F	4.7	0.03	2.6	2.1

[a] Derived from measurements at 25 °C listed in Table 2. [b] Derived from eq 5 for T_0 = 25 °C; see text. For M13Nle, the values used are listed in Table 1. For the other peptides, comparable values were obtained from Table 1 of Varadarajan et al. (1992). [c] $T\Delta\Delta S° = \Delta\Delta H - \Delta\Delta G°$.

previously (Varadarajan et al., 1992) are also included. The values for these peptides were calculated the same way as those for M13Nle and are slightly different from those reported earlier due to omission in the fitting procedure of the data at 25 °C (see Discussion).

Table 3 lists the values of the various thermodynamic binding parameters relative to the S15 peptide so that, for $\Delta J = \Delta G°$, ΔH, $\Delta S°$ or ΔC_p, $\Delta\Delta J_X = \Delta J_{M13X} - \Delta J_{S15}$. The ΔH and ΔC_p data were taken from Table 2. The $\Delta G°$(25 °C) values were obtained from the following formula applied in the temperature range 5–20 °C to the data in Table 1 of this paper or from Table 1 of Varadarajan et al. (1992):

$$\Delta G°_{bind}(T_0) = \Delta H(T_0) - T_0[[\Delta H(T) - \Delta G°(T)]/T + \Delta C_p \ln(T_0/T)] \quad (5)$$

where T_0 = 298 K. The values calculated from all data in the given temperature range were averaged and used to provide the difference values. These differences are the same within about 0.2 kcal/mol as those calculated from the values of ΔG measured at 25 °C.

Crystal Structure. The results of the final refinement are summarized in Table 4. The mutant complex crystallized in the same space group as the wild-type and other mutants at position 13 (Varadarajan & Richards, 1992), and the crystals had similar unit-cell parameters. The resolution of the present dataset (1.85 Å) is similar to that of the other mutant structures (Varadarajan & Richards, 1992). The experimental conditions for the X-ray and thermodynamic studies differ in pH and the presence of saturating sulfate bound in the active site in the crystallographic studies. However, earlier work has shown that the structures of RNase-S and RNase-A are relatively independent of pH over a wide pH range [see Kim et al. (1992) and references cited therein]. Furthermore, structures of RNase-A without phosphate and containing a uridine vanadate transition state analog bound in the active site are virtually identical, suggesting that sulfate binding does not perturb the structure of RNase-S significantly (Wlodower et al., 1988; Borah et al., 1985).

Table 4: Summary of Data and Refinement for the M13Nle Mutant of RNase S

$a = b$ (Å)	44.74
c (Å)	97.35
resolution (Å)	1.85
% unique reflections measured	88.6
average I/σ (I)	26.6
R_{merge} (%)	4.4
R_{final} (%)	17.4
rms deviations in	
bond lengths (Å)	0.008
bond angles (deg)	1.5
no. of waters	54

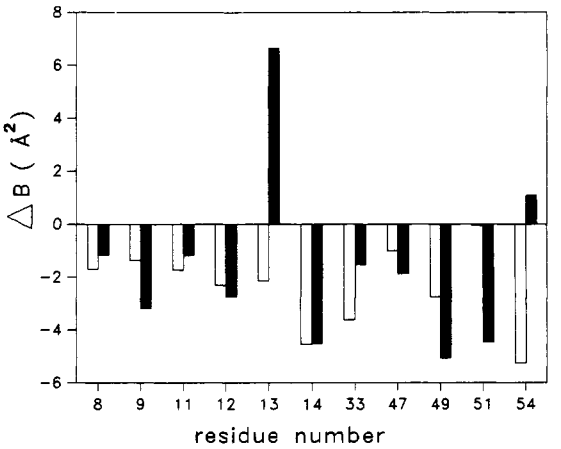

FIGURE 3: Difference in *B*-factors between the Nle complex and the wild-type Met complex for main chain (white bars) and side chain (black bars) atom group averages for residues with at least one atom at a distance of 4 Å or less from some part of residue 13.

Met13 occurs at the C-terminal end of the helix that extends from residues 3 to 13. The side chain is 94% buried and has an accessible area of 10 Å^2 (Lee & Richards, 1971). The electron density for Met13 is clearly defined and the side chain was modeled in a single conformation with dihedral angles χ_1, χ_2, and χ_3 of −69°, −57° and −53°. In the M13Nle complex, the electron density for Nle 13 is also clearly defined, and the side chain dihedral angles are essentially identical to the wild-type values. The average *B*-factor of side chain atoms is significantly higher (Figure 3) for the Nle side chain relative to the wild-type Met value (22 vs 15 Å^2).

B-factor differences between X-ray data sets are often difficult to interpret because they depend on many factors including the size of the crystal and the amount of radiation damage as well as static and dynamic disorder within the crystal. However, if we examine the pattern of *B*-factor differences for main and side chain atoms in van der Waals contact with residue 13, it is quite striking. All of these residues in the M13Nle complex have lower *B*-factors than the same residues in the wild-type complex except for Val 54 which shows a small increase. In contrast, the *B*-factors for residue 13 itself are much larger with Nle than with Met in that position. Thus, although absolute *B* values in different data sets may be uncertain, one can be more confident about differences between paired groups. In this case, the changes between the cage groups surrounding residue 13 tend to go in one direction while the side chain atoms of residue 13 itself go in the other. This difference in behavior would be true regardless of the absolute relation of the two *B*-factor sets.

Table 5: Residues Found in Two Conformations

residue	conf	B	q	χ_1	χ_2	χ_3	χ_4	χ_5
Met29	1	19	0.48	−158	58	73		
	2	10	0.52	−76	−64	−80		
Ser32	1	47	0.48	−62				
	2	21	0.52	−179				
Leu35	1	12	0.61	−60	−58			
	2	8	0.39	−72	−141			
Val43	1	9	0.38	56				
	2	16	0.62	−55				
Ser77	1	31	0.74	57				
	2	12	0.26	−175				
Asp83	1	34	0.51	173	−97			
	2	13	0.49	−63	−89			
Arg85	1	27	0.38	−171	160	−67	95	180
	2	11	0.62	−179	170	−68	−106	−179

Although the data in Figure 3 were generated using unrestrained B-factor refinement, identical trends are seen if restrained B-factor refinement, with the restraints described under Materials and Methods, was carried out instead. Attempts were therefore made to model the Nle side chain in two conformations. However, no significant electron density was seen for a second conformation in either the $2F_o - F_c$ or the $F_o - F_c$ electron density maps whether or not a second conformation was included in the model. Hence, Nle13 exists in a single conformation very similar to that of Met13 in the wild-type complex, but has somewhat greater mobility. No similar change in B-factors is observed for other mutants previously studied (Varadarajan & Richards, 1992). In those cases, there are increases as well as decreases in B-factors for residue 13 as well as surrounding residues relative to corresponding wild-type values, and no clear trend is discernible.

Seven other side chains were modeled in two conformations in the Nle complex (see Table 5). In contrast to Nle itself, for all of these cases the $2F_o - F_c$ and $F_o - F_c$ maps showed clear peaks at the contour levels mentioned above when only a single conformation was included in the model. After inclusion of the second conformation, the positive peaks in the difference map disappeared, and no new negative peaks appeared. All of these residues are also found in multiple conformations in the wild-type complex (Kim et al., 1992).

Shown in Figure 4 are the average rmsd's, relative to the wild-type complex, of the main and side chain atoms as a function of residue number. The only side chains that have rmsd's of greater than 1 Å are Lys7, Gln28, Lys31, Arg39, Lys66, Lys104, and Asn113. These are all disordered residues with high B-factors and poorly defined electron densities in both wild-type and mutant structures; hence, the observed differences at these positions are not significant. Replacement of the SD atom in Met by a methylene group in Nle results in a change in the CG–XD and XD–CE bond lengths from 1.8 to 1.5 Å and a change in the CG–XD–CE bond angle from 101 to 111°. Shown in Figure 5 is a slice through a region of the protein surrounding residue 13. Shown in Figure 6 are displacements of the mutant N, C, and CA atoms as a function of distance from the CA atom of residue 13. The largest changes in main chain atom positions occur for residues 65–70 and 88–90, which are in loop regions, and residue 123, which is close to the C-terminus (see Figures 5 and 6). None of these atoms are in van der Waals contact with residue 13 and are in fact more than 15 Å from the site of mutation. Similar patterns were previously observed in several other mutants at position 13 (Varadarajan & Richards, 1992), but at the present time, we have no explanation for these

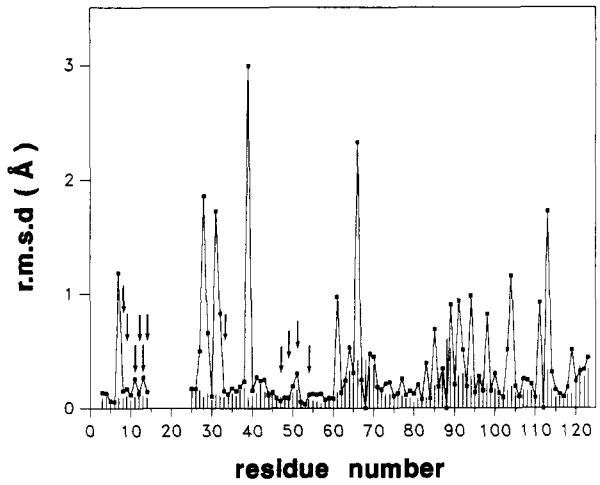

FIGURE 4: Root mean square deviation in the main chain (vertical lines) and side chain (■) atoms between the Nle and Met complexes. Residues with any atom within 4 Å of any atom in residue 13 are indicated by arrows. The two proteins were superposed by least squares so as to minimize deviations between corresponding main chain atoms. The disordered residues 1–2, 15, 21–24, and 124 were omitted from the superposition procedure and from the figure.

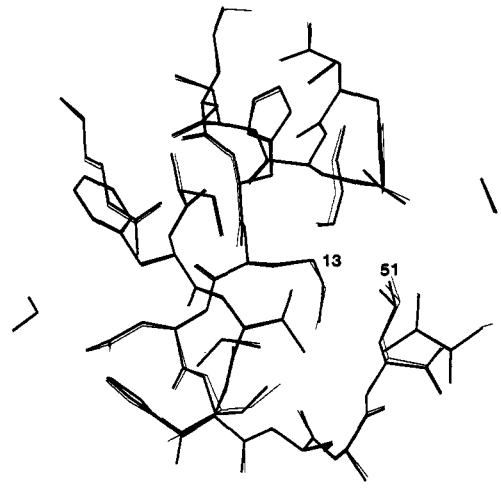

FIGURE 5: Slice through the region surrounding residue 13. The complexes, Nle variant (thick line) and wild-type Met (thin line), were superposed as described in the legend of Figure 4. Residues 13 and 51 have been numbered.

observations. Thus, apart from the changes in the loop regions, the only significant difference between the Met and Nle complexes is an increase in the average B-factor for the Nle side chain versus Met13.

DISCUSSION

For temperatures in excess of 25 °C, the fraction of peptide that assumes a helical conformation is negligible (Mitchinson & Baldwin, 1986; Connelly et al., 1990), and no correction for fractional helicity need be considered. On the basis of the temperature dependence of the mean residue ellipticity data of Connelly et al. (1990), it would appear that at 5 °C about 7% of the S15 peptide would assume a helical conformation. On the basis of DSC studies of an alanine-rich 50-residue peptide, the enthalpy for a helix–coil transition is estimated to be 0.9–1.3 kcal/mol of residue (Scholtz et al., 1991). Since residues 3–13 of S15 assume a helical conformation in RNase-S (Varadarajan et al., 1990), the enthalpy associated with this helix–coil transition would be estimated to account for 10–14 kcal/mol of the total enthalpy of the binding reaction. Connelly and Wemmer (personal communication) have

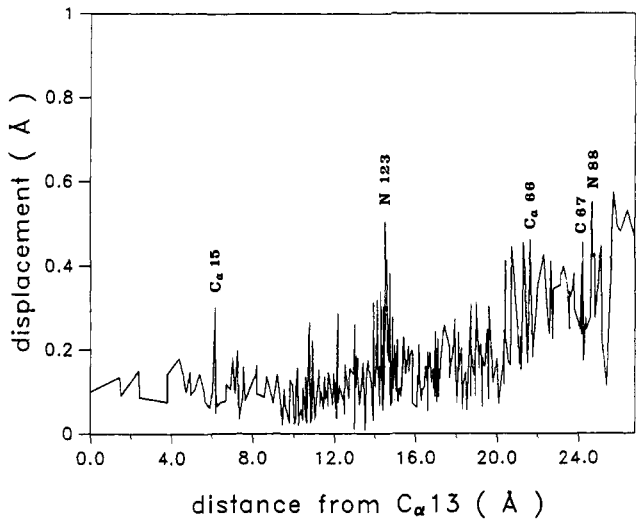

FIGURE 6: Absolute value of the difference in position of main chain atoms in the Nle complex with respect to the wild-type Met complex. The Nle and Met complexes were superposed by least squares so as to minimize the deviations between corresponding main chain C, CA, and N atoms. The disordered residues 1, 21–24, and 124 and oxygen atoms were omitted from the superposition and from the figure.

studied the binding of a disulfide-stabilized peptide designed to have a helical peptide structure at room temperature. Their results suggest that the helix–coil transition accounts for about 10 kcal/mol of the total enthalpy of the binding reaction at 25 °C. Therefore, one would expect that in the temperature range of 5–25 °C the presence of intact helical peptide will only marginally affect the total heat of the binding reaction (≤1 kcal/mol compared to 20 –30 kcal/mol for the overall reaction). CD studies of the Nle peptide (data not shown) indicate that it behaves like the wild-type and other S-peptide analogs previously studied (Connelly et al., 1990). At 5 °C, it has similar helicity to the other peptide analogs (<10%) while at 25 °C it is essentially a random coil.

Similarly, at temperatures in excess of 25 °C, it is inappropriate to assume that all of the free S-protein in solution will assume the native state (Tsong et al., 1970; Hearn et al., 1971; Varadarajan et al., 1992). On the basis of the data in Figure 4 of Varadarajan et al. (1992), approximately 50% of the free S-protein molecules will be in the denatured state at 40 °C. In contrast to the case of the presence of intact helical peptide at lower temperatures, the presence of unfolded S-protein will have a significant effect on the total heat of the binding reaction due to the large ΔH of unfolding.

Figure 2 shows a plot of the heat of reaction of peptide with S-protein after attempting to correct for the perturbation of the equilibrium between denatured and free native state S-protein. These values were obtained by fitting the observed heats of reaction, $\Delta H_{obs}(T)$, to the equation:

$$\Delta H_{calc}(T) = \Delta H_{obs}(T) - f_u(T)[\Delta H_{fold}(T_{1/2}) + \Delta C_{pfold}(T - T_{1/2})] \quad (6)$$

where $\Delta H_{calc}(T)$ is the enthalpy of binding at temperature T calculated as indicated in eq 2, $f_u(T)$ is the fraction of unfolded S-protein at temperature T, $\Delta H_{fold}(T_{1/2})$ is the heat of refolding of S-protein at the temperature of half-conversion, $T_{1/2}$, and ΔC_{pfold} is the heat capacity change for the folding of S-protein. In fitting the data, ΔH_{calc} was assumed to be linearly dependent on temperature (i.e., ΔC_{pbind} is assumed to be independent of temperature). To reduce the number of adjustable parameters a temperature-independent value of 1.4 kcal mol^{-1} K^{-1}, as reported by Hearn et al. (1971), was used for ΔC_{pfold}. This value, obtained at pH 7.0, was also assumed to be independent of pH [Privalov et al., 1989; see p 222 of Privalov (1979)]. The fraction of denatured protein at each temperature was calculated as

$$f_u(T) = K_{eq}(T)/[K_{eq}(T) + 1] \quad (7)$$

with

$$K_{eq}(T) = \exp[-\Delta G°(T)R^{-1}T^{-1}] \quad (8)$$

and

$$\Delta G°(T) = \Delta H_{fold}(T_{1/2})(1 - T/T_{1/2}) - \Delta C_{pfold}[T_{1/2} - T + T\ln(T/T_{1/2})] \quad (9)$$

$\Delta H_{fold}(T_{1/2})$ and $T_{1/2}$ were varied until the minimum linear least-squares deviation of a plot of $\Delta H_{calc}(T)$ versus temperature was achieved. The best-fit value of $\Delta H_{fold}(T_{1/2})$, –49.0 kcal/mol, falls in the range of –43 to –63 kcal/mol reported by Hearn et al. (1971) for the unfolding of S-protein at pH 7. The differential scanning calorimetric (DSC) curve obtained for S-protein is much broader than that for RNase-S [see, for example, Figure 4 in Varadarajan et al. (1992)]. The inherent difficulty presented in analyzing broad DSC curves gives rise to the large variation in $\Delta H_{fold}(T_{1/2})$ reported by Hearn et al. (1971). The best-fit value of $T_{1/2}$, 39.9 °C, correlates with the maximum of the S-protein denaturation profile, 42 °C, published by Varadarajan et al. (1992).

By assuming that the heat capacity for the binding reaction, ΔC_{pbind}, is independent of temperature, the data presented in Figure 2 can also be used to obtain ΔC_{pbind} and an estimate of $\Delta H_{bind}(T_0)$ from the equation:

$$\Delta H_{calc}(T) = \Delta H_{bind}(T_0) + \Delta C_{pbind}(T - T_0) \quad (10)$$

The values of $\Delta C_{pbind}(T_0)$ and $\Delta H_{bind}(T_0)$ obtained from this procedure are 1.0 ± 0.6 kcal mol^{-1} K^{-1} and –34 kcal/mol, respectively, which, within error, agree with the values obtained using only the 5–20 °C data.

Both Spolar et al. (1992) and Murphy et al. (1992) suggest that the heat capacity change upon protein folding can be estimated from the amounts of polar and nonpolar accessible surface area buried upon folding based on a balance between the burial of polar surface area with a positive heat capacity change and the burial of nonpolar surface area with a negative heat capacity change. However, recent studies by Makhatadze and Privalov (1990, 1993) and Privalov and Makhatadze (1990, 1993) indicate that factors other than side chain solvation must be involved.

The sulfur atom in Met is more polar and less hydrophobic than the corresponding methylene group in Nle. Hence, in the present study, it would be expected that the M13Nle, M13I, and M13L peptides would have more negative ΔC_ps of binding than the Met-containing peptide. However the results in Tables 2 and 3 clearly indicate otherwise. This confirms our earlier assertion (Varadarajan et al., 1992) that other factors besides the burial of surface area contribute to the observed ΔC_p of protein folding.

Methionine is the longest unbranched nonpolar amino acid and has an unusually flexible side chain. In a recent attempt to understand this flexibility, Gellmann (1991) analyzed the conformational differences previously observed between butane and thiobutane in the gas phase. Butane shows a distinct preference for the anti over the gauche conformation (H_{anti}

$-H_{gauche} = -0.8$ kcal/mol). In contrast, in thiobutane the gauche conformation is slightly favored, $H_{anti} - H_{gauche} = 0.05 \pm 0.2$ kcal/mol. The reason for this slight preference for the gauche conformation in thiobutane is not known. The C–S bond is 0.3 Å longer than the corresponding C–C bond. This leads to a decrease in the steric repulsion between the terminal methyl groups in the gauche conformation of thiobutane relative to the repulsion in the gauche conformation for butane. It is suggested that this effect is partly responsible for the preference for the anti conformation in butane.

However, for Nle in the M13Nle complex, the observed side chain dihedral angles χ_1, χ_2, and χ_3 are −69°, −60°, and −53°, respectively. Since the Nle side chain had a significantly higher *B*-factor than Met13 we attempted to include a second conformation with dihedral angles of −69°, −60°, and −180°. This conformation can be accommodated without any steric overlap with other atoms within the protein. However, after refinement using simulated annealing, the first conformation was practically unchanged while no electron density was visible for the second conformation. Hence, in subsequent refinement only the first conformation was retained. Therefore, unlike butane, the gauche conformation is favored over the anti about the CG–CD bond in Nle13. The reason for this is not obvious since in both conformations the residue has a similar van der Waals energy of interaction with other residues within the protein as well as a similar solvent accessible area. Since the space to accommodate both conformers appears to be available, it is curious that they are not both seen.

The increased *B*-factor for Nle13 is indicative of an increase in mobility for this residue. This is qualitatively consistent with the positive observed $T\Delta\Delta S$. Isotropic *B*-factors have been used in the refinement. These may be interpreted as proportional to mean square displacements of the atom centers. The latter in turn, to the 3/2 power, will be proportional to volume fluctuations. The entropy difference between two states, otherwise identical, will be proportional to the log of the ratio of such volumes, or $T\Delta S = RT \ln(B_{Nle}/B_{Met})^{3/2}$. This very crude estimate is less than 1 kcal/mol, comparable to the estimate based on two conformers vs one which would be RT ln 2 or 0.4 kcal/mol. Hence, such factors can only account for a small fraction of the observed $T\Delta\Delta S$ of 7.3 kcal/mol (Table 3). No estimate has been made yet on the difference in vibrational behavior and associated entropy change between the alkane and thioether side chains.

Since the structures of the two complexes are very similar, the large changes in enthalpy and entropy may be due to (1) differences in the hydration of the free peptides, (2) differences in the electrostatic interaction energies of Met and Nle in the respective complexes, or (3) differences in the overall dynamic behavior of the complexes, or some combination of all (1)–(3). We are currently carrying out molecular dynamics simulations as well as experimental measurements of the dynamics via tritium exchange studies in order to test these hypotheses.

ACKNOWLEDGMENT

We express our appreciation for discussions and help from P. R. Connelly. We thank the following units at the Indian Institute of Science for advice and use of their equipment: Area Detector Facility located at the Molecular Biophysics Unit, Interactive Graphics Facility, and Supercomputer Education and Research Center. In New Haven, our thanks go to the W. M. Keck Foundation, Biotechnology Resource Laboratory of Yale University. We also thank the two referees of this paper, who obviously read it with great care. Almost all of their comments are included in the revised version of the original manuscript.

REFERENCES

Borah, B., Chen, C., Egan, W., Miller, M., Wlodower, A., & Cohen, J. S. (1985) *Biochemistry 24*, 2058–2067.
Brünger, A. T. (1992) *X-Plor Version 3.1*, Yale University Press, New Haven, CT.
Connelly, P. R., Varadarajan, R., Sturtevant, J. M., & Richards, F. M. (1990) *Biochemistry 29*, 6108–6114.
Doscher, M. S., & Hirs, C. H. W. (1967) *Biochemistry 6*, 303–312.
Gellmann, S. H. (1991) *Biochemistry 30*, 6633–6636.
Hearn, R. P., Richards, F. M., Sturtevant, J. M., & Watt, G. D. (1971) *Biochemistry 10*, 806–817.
Howard, A. J., Neiber, C., & Xuong, H. N. (1985) *Methods Enzymol. 114*, 452–472.
Jones, T. A. (1985) *Methods Enzymol. 115*, 157–171.
Kim, E. E., Varadarajan, R., Wyckoff, W. H., & Richards, F. M. (1992) *Biochemistry 31*, 12304–12314.
Lee, B., & Richards, F. M. (1971) *J. Mol. Biol. 55*, 379–400.
Makhatadze, G. I., & Privalov, P. L. (1990) *J. Mol. Biol. 213*, 375–384.
Makhatadze, G. I., & Privalov, P. L. (1993) *J. Mol. Biol. 232*, 639–659.
Mitchinson, C., & Baldwin, R. L. (1986) *Proteins: Struct., Funct., Genet. 1*, 23–33.
Murphy, K. P., Bhakuni, V., Xie, D., & Freire, E. (1992) *J. Mol. Biol. 227*, 293–306.
Privalov, P. L. (1979) *Adv. Protein Chem. 33*, 167–241.
Privalov, P. L., & Makhatadze, G. I. (1990) *J. Mol. Biol. 213*, 385–391.
Privalov, P. L., & Makhatadze, G. I. (1993) *J. Mol. Biol. 232*, 660–679.
Privalov, P. L., Tiktopulo, E. I., Venyaminov, S. Yu., Griko, Yu. V., Makhatadze, G. I., & Khechinashvili, N. N. (1989) *J. Mol. Biol. 205*, 737–750.
Scholtz, J. M., Marqusee, S., Baldwin, R. L., York, E. J., Stewart, J. M., Santoro, M., & Bolen, D. W. (1991) *Proc. Natl. Acad. Sci. U.S.A. 88*, 2854–2858.
Spolar, R. S., Livingstone, J. R., & Record, T. M., Jr. (1992) *Biochemistry 31*, 3947–3955.
Tsong, T. Y., Hearn, R. P., Wrathall, D. P., & Sturtevant, J. M. (1970) *Biochemistry 9*, 2666–2677.
Varadarajan, R., & Richards, F. M. (1992) *Biochemistry 31*, 12315–12327.
Varadarajan, R., Richards, F. M., & Connelly, P. C. (1990) *Curr. Sci. 59*, 819–824.
Varadarajan, R., Connelly, P. R., Sturtevant, J. M., & Richards, F. M. (1992) *Biochemistry 31*, 1421–1426.
Wiseman, T., Williston, S., Brandts, J., & Lin, L. (1989) *Anal. Biochem. 179*, 131–137.
Wlodawer, A., Svenson, L., Sjolin, L., & Gilliland, G. L. (1988) Biochemistry *27*, 2705–2717.